On reverse gate leakage current of GaN high electron mobility transistors on silicon substrate

Ling Xia,[1] Allen Hanson,[1] Timothy Boles,[1] and Donghyun Jin[2]
[1]*M/A-COM Technology Solutions, Inc., 100 Chelmsford Street, Lowell, Massachusetts 01851, USA*
[2]*Massachusetts Institute of Technology, 77 Massachusetts Avenue, Massachusetts 02139, USA*

(Received 21 November 2012; accepted 12 March 2013; published online 21 March 2013)

Reverse leakage current characteristics of Ni Schottky contacts to GaN grown on Si is experimentally studied using high electron mobility transistors (HEMT). The temperature in this study is between 273 K and 428 K. The reverse gate leakage current is found to be dominated by Frenkel-Poole emission, a trap-assisted process, when the reverse electric field is smaller than 1.4 MV/cm. For electric field larger than 1.6 MV/cm, the underlying mechanism is mainly Fowler-Nordheim tunneling, an electric-field-dominated process. As a result, properly engineering electric field is considered critical for reducing reverse leakage current in GaN-on-Si HEMT for high-voltage applications. © *2013 American Institute of Physics*. [http://dx.doi.org/10.1063/1.4798257]

Recently, GaN grown on silicon substrates has attracted great interest for applications in high-voltage power electronics.[1–4] Among many merits, the combination of high breakdown voltages in GaN transistors and the low cost of silicon substrates is extremely desirable of GaN-on-Si epitaxial structures. GaN high electron mobility transistors (HEMT) on Si substrates have demonstrated breakdown voltages well above 1000 V.[3,4] In addition, the substrate cost of GaN on Si can be 100 times lower than conventional GaN on SiC.

For applications in high-voltage power electronics, to fully understand and to properly engineer reverse gate leakage current in GaN HEMT are important as this current can cause severe problems. For instance, in high-voltage applications, more than 1000 V can be applied across the drain and the gate of a HEMT, when the HEMT is in off state. The associated leakage current levels must remain low enough (preferably $< 1\ \mu$A/mm) to ensure reasonable off-state power dissipation as well as successful voltage blocking.

Past experimental studies have revealed important mechanisms of reverse leakage current in Ni-GaN Schottky contacts for GaN on SiC or sapphire substrates.[5–8] Nevertheless, the reverse electric fields in these studies are relatively low with respect to the range of particular interest for power electronics applications, partly because the structures chosen for the studies are diodes with large circular diameters ($>100\ \mu$m).[5–8] For these large diodes, the electric field under the anode only increases to a certain level. After that, the additional voltage applied to the anode drops mainly between the anode electrode edge and the cathode contact. Thus, the electric field in the major area underneath the anode electrode remains almost unchanged in these large diodes. As a result, the leakage current changes little in a wide range of reverse voltages after it is above a certain level.[7]

This paper reports a study on mechanisms of reverse gate leakage current in a GaN on Si structure, through temperature dependences of reverse current of Ni-GaN Schottky contacts. Instead of circular diode structures, HEMT is employed to perform the analysis. In HEMT structures, reverse electric field in the gate diode can be increased beyond the saturation level in a circular diode. Therefore, studying leakage mechanisms under high electric fields is made possible.

Figure 1 shows a schematic of the devices used in this study. The epitaxial structure includes a 0.8 μm GaN channel, 18 nm AlGaN, and a 2.5 nm GaN cap on the top. Ti/Al/Ni/Au metal stack was used for ohmic contacts. After the contacts were formed, 150 nm SiN was deposited using plasma-enhanced chemical vapor deposition (PECVD) for passivation. Gate opening was defined by SF_6-based inductively coupled plasma (ICP) etch. Our controlled experiments with wet etch indicated that the GaN cap was not attacked by the ICP etch. Ni/Au was used to form the gate electrode. A post-gate anneal[9] was performed under 375 °C. A total of nine HEMTs across a 4-in. wafer was measured. The gate length, source-gate, and drain-gate distances of the HEMTs were all 1 μm, as shown in Figure 1. Current-voltage characteristic (*I-V*) were measured with the temperature ranging from 273 K to 428 K with a 25 K step. During the measurements, gate voltage was swept, drain was grounded, and source and substrate were floating. At the end of the temperature cycle, we confirmed that the *I-V* characteristics restored to their initial status. Thus, no permanent change happened in the devices during the *I-V-T* measurements.

Figure 2 shows the *I-V-T* characteristics of Ni-GaN contacts on Si. Clearly, the reverse leakage current (J_r) increases with temperature when the reverse voltage (V_r) is between 0 and −10 V. In contrast, J_r is less dependent on temperature when V_r becomes more negative than −10 V. In fact, the dependence of $\log(J_r)$ on T is not monotonic with $V_r < -10$ V.

Activation energy method[10] is used to extract the Schottky barrier height (ϕ_B) and Richardson's constant (A*) for the Ni-GaN contacts. The value of ϕ_B is 1.12 V with a standard error of less than 0.7 mV. This value is higher than reported values (0.8–0.9 V) of Ni-GaN contacts.[5,6,11,12] The main reason is attributed to the post-gate anneal, which has been found to increase ϕ_B of Ni-GaN contacts.[13,14] This is also confirmed by the fact that the threshold voltage of our HEMT shifts approximately +0.25 V after the gate anneal. It is known that a shift in ϕ_B of gate contact induces a

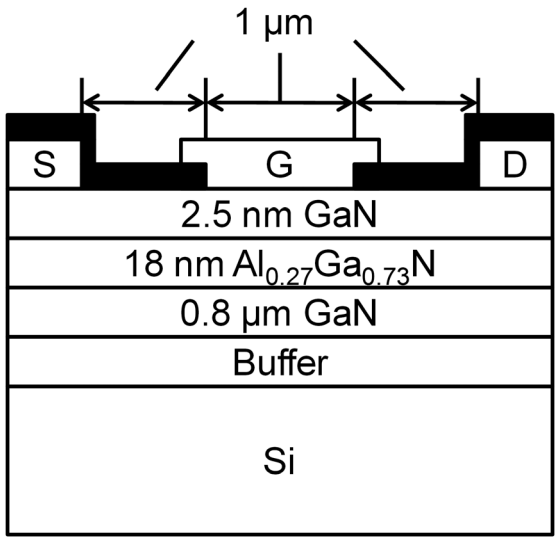

FIG. 1. Schematics of GaN high electron mobility transistors used in this study.

comparable amount of shift in the threshold voltage of HEMT.[15,16] The ideality factor, n, is 1.33 with a standard error of less than 0.01. The Richardson's constant is extracted to be 3.26 A cm^{-2} K^{-2} with a standard error of 3.91 A cm^{-2} K^{-2}. This value lies well in the range of A* reported from experiments (0.001–5.92 A cm^{-2} K^{-2}).[6,11]

The temperature dependence of J_r is critical to reveal underlying leakage mechanisms in the Ni-GaN transistors. Similar to studies on GaN on SiC or sapphire,[5–8] two mechanisms are found dominant in the Ni-GaN contacts on Si. The first one is Frenkel–Poole (FP) emission.[17,18] This emission refers to tunneling through trap states in the wide-band gap semiconductor or insulator into continuum states. The current density associated with FP emission is[5,7,8]

$$J_{FP} = CE_r \exp\left[-\frac{q(\varphi_t - \sqrt{qE_r/\pi\varepsilon_0\varepsilon_s})}{kT}\right], \quad (1)$$

where C is a constant, E_r is the reverse electric field in the AlGaN barrier, ϕ_t is the potential barrier of traps for electron emission referenced to the metal Fermi level, q is the elementary charge, k is the Boltzmann's constant, ε_s is the relative permittivity of AlGaN, and ε_0 is the vacuum permittivity.

The second dominant mechanism is considered to be Fowler-Nordheim (FN) tunneling.[19] FN tunneling increases with electric field but does not need assistances from trap states. The current density for this mechanism can be expressed as[5]

$$J_{FN} = AE_r^2 \exp\left(-\frac{B}{E_r}\right), \quad (2)$$

where A and B are constants related to material properties, and E_r again is the reverse electric field in AlGaN barrier.

Equations (1) and (2) show that FP emission is temperature-dependent, whereas FN tunneling is not. This is expected to the first order. FP emission increases with temperature because electron trapping is thermally activated. In comparison, such a trapping process is not required in FN tunneling, and therefore little temperature dependence is expected in FN tunneling. As a result, the observed temperature dependence of J_r in our experiments indicates important information: FP emission dominates J_r when V_r is larger than −7 V, whereas FN tunneling becomes dominant when V_r is below approximately −10 V.

Plotting $\log(J_r/E_r^2)$ versus $1/E_r$ and $\log(J_r/E_r)$ versus $E_r^{0.5}$ should further confirm the mechanisms responsible for the gate leakage in different voltage ranges. As can be seen in Eq. (2), $\log(J_r/E_r^2)$ is predicted to be linearly proportional to $1/E_r$ if FN tunneling is the dominating mechanism. Figure 3 shows the calculated $\log(J_r/E_r^2)$ as a function of $1/E_r$. It is clear that when $1/E_r$ is less than around 0.63 cm/MV, $\log(J_r/E_r^2)$ becomes independent on temperature and linearly proportional to $1/E_r$. In other words, when electric field (E_r) is above 1.6 MV/cm in AlGaN barrier, FN tunneling dominates the gate leakage current.

In the above calculations, E_r was obtained from two-dimensional HEMT simulations by SILVACO simulator. The simulation model was adjusted to match the two dimensional electron gas (2DEG) sheet density from Hall

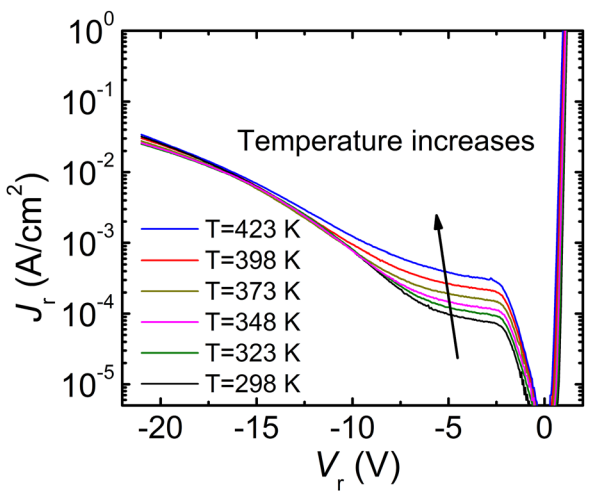

FIG. 2. Example current-voltage (I-V) characteristics of Ni contacts to GaN on silicon substrate. The temperature varies from 298 K to 423 K with a 25 K step.

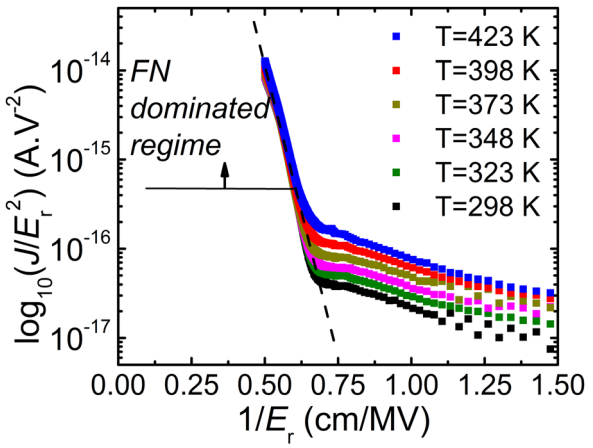

FIG. 3. An example of plotting $\log(J_r/E_r^2)$ as a function of $1/E_r$. For $1/E_r < 0.63$ cm/MV ($E_r > 1.6$ MV/cm), the variable $\log(J_r/E_r^2)$ is linearly proportional to $1/E_r$ and is independent on temperature. This is the regime dominated by FN tunneling.

measurements and the threshold voltage of our HEMTs. The 2-dimensional distribution of electric field with $V_r = -20$ V is shown in Figure 4 as an example. The reverse electric field (E_r) was taken as the average electric field in the AlGaN barrier. The plot on the right in Figure 4 shows E_r as a function of V_r. The increase of electric field is rapid at low voltage ($-2\,\text{V} < V_r < 0\,\text{V}$), followed by a lower rate after the 2DEG is depleted. In addition, negligible dependence of E_r on temperature is seen from the simulations in our temperature range. Lattice temperature in our diodes was not expected to be significantly different from the temperature set by our heating system because the diodes were in off-state and were not dissipating heat substantially.

Similarly, $\log(J_r/E_r)$ is expected to be linearly proportional to $E_r^{0.5}$ if the underlying mechanism is FP emission, as indicated by Eq. (1). Figure 5 shows $\log(J_r/E_r)$ as a function of $E_r^{0.5}$ in the range where the relation depends on temperature. Consistent with the FP tunneling model, the variable $\log(J_r/E_r)$ changes linearly with $E_r^{0.5}$, when electric field is <1.4 MV/cm. Thus, in this electric field range, the dominating mechanism is confirmed to be FP tunneling. Between 1.4 and 1.6 MV/cm, the leakage current is considered a mix of FN and FP tunneling components.

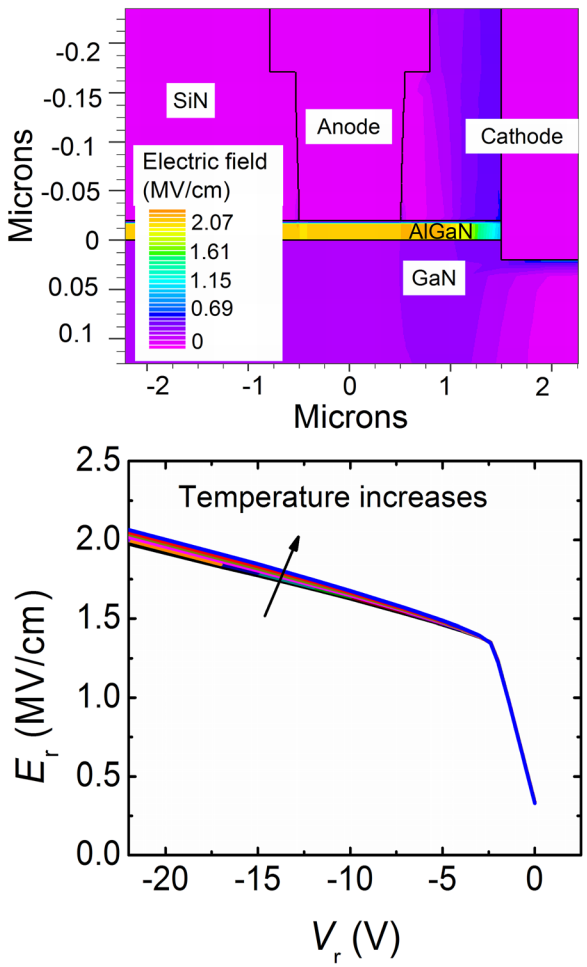

FIG. 4. (Up) Two-dimensional electric field distribution simulated by SILVACO software. $V_r = -20$ V. (Down) Dependence of E_r on V_r. The temperatures in simulations are the same as in our experiments. Negligible differences are seen in E_r in our temperature range.

The trap energy level ($E_t = q\phi_t$) associated with the FP tunneling process can be extracted from Eq. (1) and Figure 5. This E_t value is the energy difference between the trap level and gate metal Fermi level. Our results show that the values of E_t are clustered into two groups: five HEMTs show $E_t = 0.23 \pm 0.02$ eV, whereas the other four show $E_t = 0.63 \pm 0.03$ eV. The data shown in Figures 2, 3, and 5 are with $E_t = 0.63$ eV. The different values of E_t are not likely caused by measurement variations because the ϕ_B, n, and A* extracted from the forward characteristics are extremely uniform for the two groups of HEMTs all together. We suspect that the two levels of ϕ_t are due to different traps in the epitaxial structure. Even for one GaN epi-structure, multiple trap levels can be found.[5,20–25] Which trap level dominates the FP tunneling might vary with the device location across the wafer. Nevertheless, further study is needed to fully characterize the variation of traps in space and energy.

While the present methodology does not allow us to identify the location of the traps (in GaN cap, in AlGaN barrier, and/or at their interface), it is useful to compare with reported values the trap energy levels with respect to GaN/AlGaN energy bands. To do so, the ϕ_B of 1.12 V extracted above and a conduction band offset (ΔE_c) of 0.49 eV (linearly interpolated from values in Ref. 26) between GaN and $Al_{0.27}Ga_{0.73}N$ were used. According to our calculation, the two trap levels, respectively, locate 0.89 eV and 0.49 eV below the conduction band edge (E_c) of GaN or 1.38 eV and 0.98 eV below the E_c of $Al_{0.27}Ga_{0.73}N$. These energy relationships are shown in Figure 5. The two trap levels for GaN are consistent with reported trap levels on other substrates.[5,20–22] For traps in AlGaN, Zhang *et al.*[5] reported a trap level that is 0.87 eV below $Al_{0.25}Ga_{0.75}N$ E_c and Fang *et al.*[24] reported a value of 1.02 eV in $Al_{0.30}Ga_{0.70}N$. These values are close to the 0.98 eV level in our experiment, given the differences in ΔE_c between GaN and AlGaN of different Al composition. Fang *et al.*[25] observed a deep electron trap of ~1.3 eV in $Al_{0.25}GaN_{0.75}N$. This value concurs with our 1.38 eV level, again considering ΔE_c differences.

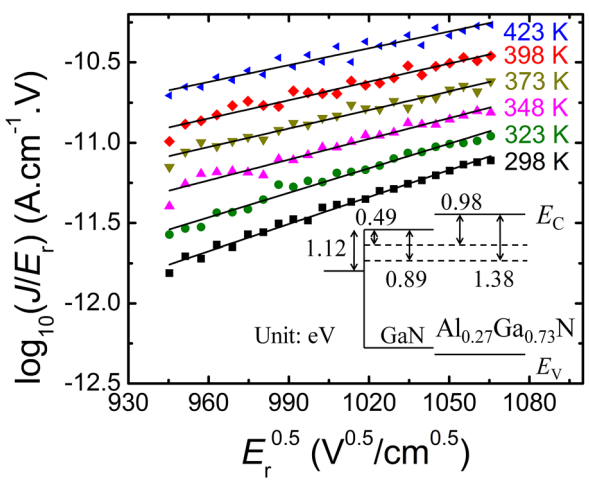

FIG. 5. An example of plotting $\log(J_r/E_r)$ as a function of $E_r^{0.5}$. Two trap levels are extracted from this type of plots for our nine HEMT samples across a 4-in. wafer. The inset schematically shows the two trap levels with respect to GaN and AlGaN conduction bands. One remark is that the location of the traps cannot be determined from the present study.

In summary, the reverse leakage current characteristics of Ni-GaN contacts on Si substrate are studied. The characteristics are obtained from the gate Schottky contacts of a GaN HEMT structure. These contacts show $\phi_B = 1.12$ V, $n = 1.13$, and $A^* = 3.26\,A\,cm^{-2}\,K^{-2}$. Our experiments show that for electric field <1.4 MV/cm, the dominating leakage current mechanism is FP emission. Two trap levels are found associated with this tunneling process in our epitaxial structure. The emission barriers of these two traps are 0.23 eV and 0.63 eV, respectively. For electric field >1.6 MV/cm, field-assisted tunneling (FN tunneling) dominates the leakage current. Given that the critical electric field for GaN is above 3 MV/cm, FN tunneling is expected to be significant for the reverse leakage current in a large range of applied voltages. As FN tunneling heavily depends on electric field, it is critical to properly engineer the reverse electric field, in order to reduce gate leakage current in GaN-on-Si HEMTs for high-voltage applications.

This work is sponsored by the GaN Electronics for Grid Applications (GIGA) program under the Department of Energy (DOE) of U.S.A.

[1]U. K. Mishra, P. Parikh, and Y. F. Wu, Proc. IEEE **90**, 1022 (2002).
[2]N. Ikeda, Y. Niiyama, H. Kambayashi, Y. Sato, T. Nomura, S. Kato, and S. Yoshida, Proc. IEEE **98**, 1151 (2010).
[3]B. Lu and T. Palacios, IEEE Electron Device Lett. **31**, 951 (2010).
[4]S. L. Selvaraj, A. Watanabe, A. Wakejima, and T. Egawa, IEEE Electron Device Lett. **33**, 1375 (2012).
[5]H. Zhang, E. J. Miller, and E. T. Yu, J. Appl. Phys. **99**, 023703-6 (2006).
[6]E. J. Miller, E. T. Yu, P. Waltereit, and J. S. Speck, Appl. Phys. Lett. **84**, 535 (2004).
[7]D. Yan, H. Lu, D. Cao, D. Chen, R. Zhang, and Y. Zheng, Appl. Phys. Lett. **97**, 153503 (2010).
[8]E. Arslan, S. Butun, and E. Ozbay, Appl. Phys. Lett. **94**, 142106 (2009).
[9]H. Kim, J. Lee, D. Liu, and W. Lu, Appl. Phys. Lett. **86**, 143505 (2005).
[10]L. Xia, W. Wu, Y. Hao, Y. Wang, and J. Xu, Appl. Phys. Lett. **88**, 152108 (2006).
[11]L. S. Yu, Q. Z. Liu, Q. J. Xing, D. J. Qiao, S. S. Lau, and J. Redwing, J. Appl. Phys. **84**, 2099 (1998).
[12]Q. Z. Liu, L. S. Yu, F. Deng, S. S. Lau, and J. M. Redwing, J. Appl. Phys. **84**, 881 (1998).
[13]N. Miura, T. Nanjo, M. Suita, T. Oishi, Y. Abe, T. Ozeki, H. Ishikawa, T. Egawa, and T. Jimbo, Solid-State Electron. **48**, 689 (2004).
[14]H. Kim, M. Schuette, H. Jung, J. Song, J. Lee, W. Lu, and J. C. Mabon, Appl. Phys. Lett. **89**, 053516-3 (2006).
[15]L. Xia and J. A. del Alamo, Appl. Phys. Lett. **95**, 243504 (2009).
[16]S. D. Mertens and J. A. del Alamo, IEEE Trans. Electron Devices **49**, 1849 (2002).
[17]J. Frenkel, Phys. Rev. **54**, 647 (1938).
[18]J. G. Simmons, Phys. Rev. **155**, 657 (1967).
[19]R. H. Fowler and L. Nordheim, Proc. R. Soc. London, Ser. A **119**, 173 (1928).
[20]T. Ito, Y. Terada, and T. Egawa, MRS Proc. **1068**, C06-09 (2008).
[21]A. Hierro, D. Kwon, S. A. Ringel, M. Hansen, J. S. Speck, U. K. Mishra, and S. P. DenBaars, Appl. Phys. Lett. **76**, 3064 (2000).
[22]A. Y. Polyakov, N. B. Smirnov, A. V. Govorkov, Z. Q. Fang, D. C. Look, S. S. Park, and J. H. Han, J. Appl. Phys. **92**, 5241 (2002).
[23]D. Jin and J. A. del Alamo, Microelectron. Reliab. **52**, 2875 (2012).
[24]Z.-Q. Fang, D. C. Look, D. H. Kim, and I. Adesida, Appl. Phys. Lett. **87**, 182115 (2005).
[25]Z.-Q. Fang, B. Claflin, D. C. Look, D. S. Green, and R. Vetury, J. Appl. Phys. **108**, 063706 (2010).
[26]I. Vurgaftman and J. R. Meyer, J. Appl. Phys. **94**, 3675 (2003).